Green Synthesis of Iron Oxide Nanoparticles incorporated with Berberine Exhibits Potent Anticancer and Antimigratory activity Against Lung Cancer Cells (A549, H460 cells) and Normal Cells (HEK-293)

Malchi Suresh[1], Kodiganti Naresh Kumar[1], Sakthivel Manju Bargavi[2], Devarajan Nalini[1*] and Tharani Munusamy[1*]
1. Central Research Laboratory, Meenakshi Academy of Higher Education and Research, Chennai-600078. Tamil Nadu, INDIA
2. Nutrition and Dietetics, Faculty of Humanities and Science, Meenakshi Academy of Higher Education and Research, Chennai-600078, INDIA
*drnalini.crl@madch.edu.in; tharaninano@gmail.com

Abstract
Traditional therapies for non-small cell lung cancer (NSCLC) are often limited by high economic burden, dose-limiting toxicity and a substantial reduction in patients' quality of life. To counteract these issues, we synthesized an eco-friendly berberine-incorporated iron-oxide nanoparticle (BR-IONPs) from an aqueous extract of P. amarus. The plant-mediated synthesis of nanoparticles was confirmed using UV–Visible spectroscopy, TEM, which confirmed the structural and morphological properties of nanoparticles. Anticancer activity on HEK-293 cells demonstrated minimal cytotoxicity in IONPs, BR and BR-IONPs whereas cisplatin exhibited high toxicity.

Notably, the berberine incorporated iron oxide nanoparticles (BR-IONPs) showed strong and selective cytotoxicity against A549, H460 NSCLC cells, with significantly lower toxicity than that of the individual components including cisplatin. A scratch-wound assay also confirmed that the (BR-IONPs) inhibited A549, H460 cell migration significantly, indicating their antimigratory ability. Collectively, these in vitro results suggest that green-synthesized BR-IONPs offer higher therapeutic value compared to the traditional chemotherapeutic drug cisplatin. Subsequent in vivo experiments are required to identify its pharmacokinetics, systemic toxicity and antitumour activity before proceeding towards preclinical development. Further studies on cell signalling and apoptosis are needed to understand how BR-IONPs trigger cancer cell death.

Keywords: Iron oxide nanoparticles, Berberine, Non-small cell lung cancer, Cisplatin.

Introduction

Lung cancer continues to be a predominant cause of cancer-related mortality worldwide, with non-small cell lung cancer (NSCLC) accounting for approximately 85% of all cases. According to GLOBOCAN 2020, lung cancer ranked as the second most frequently diagnosed cancer and the foremost cause of cancer fatalities globally, with an estimated 2.2 million new diagnoses and 1.8 million deaths each year [6]. Cigarette smoking accounts for nearly 80% of fatalities associated with lung cancer, establishing it as the foremost risk factor. Other contributing factors encompass exposure to radon, radioactive substances, industrial carcinogens, air pollution and genetic susceptibility. Early-stage lung cancer can be efficiently treated with surgical resection and targeted therapies.

However, in advanced stages, delayed diagnosis and nonspecific symptoms pose major therapeutic challenges, frequently leading to poor prognosis and limited treatment options. Moreover, treatment resistance, influenced by factors such as alterations in the tumour microenvironment and genetic mutations, significantly impacts therapeutic efficacy and contributes to disease progression[13,14].

Nanotechnology has surfaced as a promising strategy in treating cancer, facilitating targeted drug delivery, minimizing systemic toxicity and improving the effectiveness of therapeutic outcomes [10]. Unlike traditional chemotherapeutic agents, which often cause severe side effects, nanotechnology-based approaches are successful even in difficult conditions and help to overcome treatment resistance, improving patient survival and quality of life[11]. The green synthesis method has various advantages over traditional chemical and physical methods including cost-effectiveness, non-toxicity, environmental friendliness and making it suitable for large-scale nanoparticles production.

Unlike conventional methods, it does not necessitate high pressure, temperature and high energy input[34]. *P. amarus*, a herb from the Euphorbiaceous family, has been used in Ayurveda for over 2,000 years and is well known for its hepatoprotective, antioxidant, antimicrobial and anticancer properties. It contains rich bioactive phytochemicals such as quercetin, kaempferol, rutin and lignans. *P. amarus* functions as both a reducing and stabilizing agent in the synthesis of nanoparticles[28].

Among nanoparticles, iron oxide nanoparticles have garnered attention due to their biocompatibility, biodegradability, non-toxicity, cost-effectiveness and magnetic properties, making them highly suitable for cancer

detection. Berberine, a natural quinoline alkaloid compound extracted from *Coptis chinensis* and various berberis species, exhibits a broad range of pharmacological activities. It has shown promising effects in treating cancer as well as in digestive, metabolic, cardiovascular and neurological disorders[12]. It functions by inhibiting pathogens, protecting vital organs such as the liver and intestines, regulating metabolic processes, enhancing cardiovascular health and providing neuroprotective benefits. Additionally, it improves the efficacy and safety of chemoradiotherapy[9,12].

Recent studies have demonstrated that berberine exerts potent anticancer effects through multiple molecular mechanisms. In lung cancer, it promotes cell death through the activation of the Bax/Bcl-2 pathway and the subsequent activation of caspase. Additionally, it halts the cell cycle by downregulating the expression of cyclin D1 and cyclin-dependent kinases (CDKs), thereby inhibiting cell proliferation[9,12]. Furthermore, it also reduces metastatic potential by inhibiting epithelial-mesenchymal transition, a key process in cancer cell invasion and metastasis. Moreover, berberine disrupts key oncogenic signalling pathways, including PI3K/Akt and MAPK/ERK pathways, which are frequently dysregulated in lung cancer.

Additionally, inhibiting NF-kB activation and reducing reactive oxygen species levels help to prevent inflammation and oxidative stress-induced cellular damage, further enhancing its overall anticancer efficacy[19,25]. Although several studies have confirmed the significant therapeutic potential of berberine, its clinical application is greatly restricted due to several limitations including poor absorption, short biological half-life, formation of inactive metabolites and quick elimination from the body, all of which significantly reduce its systemic bioavailability[25].

To address these limitations, nanotechnology-based drug delivery systems, particularly iron oxide nanoparticles, have surfaced as a viable approach to enhance the therapeutic efficacy of berberine. The present study aims to develop a green synthesis of berberine-incorporated iron oxide nanoparticles (BR-IONPs) and to evaluate their anticancer and anti-migratory effects against non-small cell lung cancer A549, H460 cells. Additionally, the cytotoxicity of nanoparticles was assessed in normal human embryonic kidney HEK-293 cells to determine biocompatibility. Cisplatin was used for positive control.

Material and Methods

Green Synthesis of *Phyllanthus amarus*-Mediated Berberine-Loaded Iron Oxide Nanoparticles: The freshly collected *Phyllanthus amarus* plants were thoroughly washed with distilled water, cut into smaller fragments, shade-dried and ground into a fine powder using a manual grinder. 10 grams of the powder were mixed with 50 mL of double-distilled water and boiled at 60°C for 30 minutes. Then, 50 mL of the *P. amarus* extract was added to 50 mL of 20 mmol $FeCl_3$ solution. The mixture was placed in an orbital shaker at 500 rpm overnight, maintaining a neutral pH.

Separately, 100 mg of berberine chloride was dissolved in 2 mL of dimethyl sulfoxide (DMSO) and diluted with 2 mL of phosphate-buffered saline (PBS) to make a final volume of 5 mL. This solution was stirred on a magnetic stirrer for 1 hour. Then, 10 mL of the berberine solution was mixed with 10 mL of the previously prepared iron *P. amarus* extract solution and subjected to sonication for 30 minutes. The mixture was placed in a hot air oven at 60°C for 1 hour. The final dried powder was collected for characterization and biological application [31] (Figure 1).

Characterization of BR-IONPs: The synthesized BR-IONPs were confirmed through various characterization techniques such as UV-visible spectroscopy (SHIMADZU UV-1900), which was performed within a wavelength range of 200-700 nm. High-resolution Transmission Electron Microscopy (HR-TEM) (Model: F200S, Thermo Fisher Scientific) was used to examine the morphology and size of the nanoparticles.

Figure 1: Green Synthesis of *Phyllanthus amarus*-Mediated Berberine-Loaded Iron Oxide Nanoparticles

Cell culture: The human A549, H460 NSCLC and HEK-293 normal lines were obtained from the National Centre for Cell Science (NCCS) located in Pune, India. The cells were maintained in Dulbecco's Modified Eagle's Medium (DMEM), which was enriched with 10% heat-inactivated Fetal Bovine Serum (FBS) and 5% Penicillin-streptomycin (10,000 U/mL). The culture was incubated at 37°C with 5% CO_2 until 90% confluence[18,19].

Cytotoxicity Assay: The MTT assay was used to investigate the cytotoxic potential of IONPs, BR, BR-IONPs and cisplatin on A549, HEK-293 NSCLC and HEK-293 cell lines. Cells were seeded into a 96-well plate at 5×10^6 cells and incubated for 24 hours. Cells were treated with various concentrations 0,25,50,75 and 100 µg/ml, in a CO_2 incubator for 24 hours. Media were discarded and replaced with 110µL of fresh media along with SDS-HCl solution and kept for 4 to 18 hours. The absorbance was noted at 570 nm using an ELISA reader. All tests were done in triplicate and the percentage of cell viability was measured [30,33].

Wound Healing Assay: A wound healing assay was performed to evaluate the migration capacity of A549, H460 NSCLC cells. Approximately 5 x 10^6 cells were seeded in a 6-well plate, supplemented with media and incubated for 24 hours. 200 µL of microtip was used to create a homogenous scratch; detached cells were removed using PBS. The cells were exposed to BR-IONPs at various concentrations 0,25,50,75 and 100 µg/mL, incubated for 24 hours. The inverted microscope was used to measure the cell migration. Each experiment was conducted in triplicate and the percentage of wound closure was measured[17,18].

Statistical Analysis: Experiments were performed in triplicate (n=3), with data entered into Microsoft Excel for analysis using SPSS (version 26, IBM, Chicago, USA). Continuous variables were reported as mean ± standard deviation (SD). Parametric tests were used since the data followed a normal distribution. A paired t-test was applied for intra-group comparisons and one-way ANOVA was used for inter-group comparisons. A significance level of 5% was set, with p-values <0.05 considered statistically significant.

Results and Discussion

Synthesis and Characterization of BR-IONPs: IONPs were successfully biosynthesized using an aqueous extract of *P. amarus*, which acted as a natural reducing and capping agent, supporting a green synthesis approach. The formation of BR-IONPs was visually indicated by a distinct colour change from yellow to dark brown, indicating the successful formation of iron oxide nanoparticles. The phytochemicals present in the plant extracts, such as phenolics, flavonoids and carotenoids, served as natural reducing and capping agents, stabilizing the nanoparticles[4]. Similar observations were reported in previous studies[8,21,22,29]. Likewise, comparable results were observed in *Phyllanthus emblica,* as confirmed by the black-coloured product[15].

Additionally, the use of *Psidium guajava* leaf extract, *Thymus migricus* and *Phoenix dactylifera* extracts produced distinct colour changes, confirming the formation of nanoparticle[3,4,8,28]. Compared with conventional approaches, the green synthesis approaches have several advantages, such as being eco-friendly, biocompatibility, stable, biodegradable, non-toxic and cost-effective in production [2].

The UV-Visible spectroscopy was employed to assess the optical properties of BR-IONPs. The absorption spectrum of displayed nanoparticles exhibited absorption peaks in the 300-350nm range, corresponding to the characteristic π–π* electronic transitions of berberine. The shift in the absorption peak compared to pure berberine suggests successful conjugation of berberine with IONPs, confirming the interaction between the organic and inorganic components[22] (Figure 2). Many studies observed similar peaks at 297 nm and 272 nm, confirming successful formation of iron oxide nanoparticles within this spectral range[17]. UV-visible absorption spectroscopy had the nearest absorption peak of berberine nanoparticles (BBR-NPs) at 344 nm.

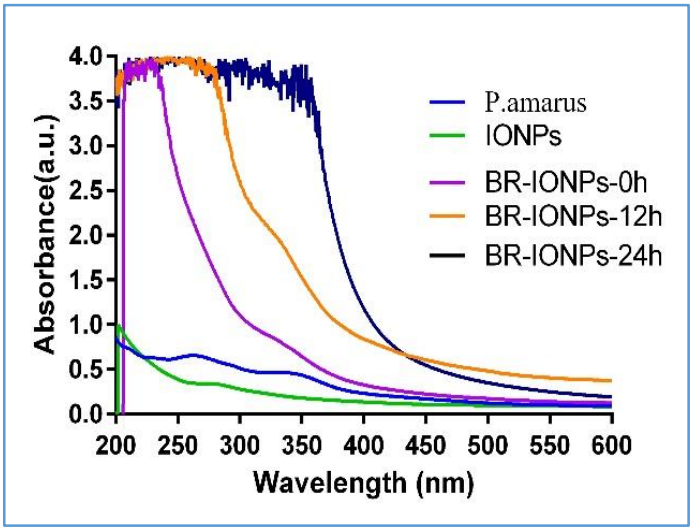

Figure 2: UV-Visible spectroscopy of BR-IONPs

TEM exhibited a rod-shaped morphology of BR-IONPs with a well-defined size distribution range between 30 and 40 nm. The uniform dispersion and shape suggest controlled synthesis with minimal aggregation. The observed morphology and size are consistent with iron oxide nanoparticles, indicating a stable conjugation with berberine (Figure 3). However, another study also confirmed the presence of rod-shaped iron oxide nanoparticles synthesized using *Moringa oleifera* leaf extract. The nanoparticles range from 10 to 90 nm, with a minimum size of 15.01 ± 6.03 nm[1]. Similarly, rod-shaped structures were observed within the 25 to 100 nm range, with an average size of approximately 9 nm[25].

Anti-Migratory Effects of BR-IONPs on A549, H460 NSCLC: The anti-migratory effect of BR-IONPs on A549 and H460 non-small cell lung cancer cell lines was evaluated using a scratch wound-healing assay, with cisplatin serving as a positive control. Cells were treated with increasing concentrations of BR-IONPs (0, 25, 50, 75 and 100 µg/mL) and incubated for 24 hours. The results demonstrated a dose-dependent inhibition of cell migration in both cell lines. In untreated control groups, a high percentage of wound closure was observed, indicating active migration. Following treatment, wound closure was significantly inhibited in a concentration-dependent manner from 21.99% at 25 µg/mL to 11.14% at 100 µg/mL in A549 cells, compared to 13.09% in cisplatin-treated cells.

Similarly, in H460 cells, wound closure decreased from 23.99% at 25 µg/mL to 12.14% at 100µg/mL, with cisplatin showing 13.87% inhibition. These findings confirm that BR-IONPs effectively suppress the migratory potential of NSCLC cells in a dose-dependent manner. The reduction in cell migration was statistically significant ($p < 0.001$), as shown in figure 4 and 5 and table 1 and 2.

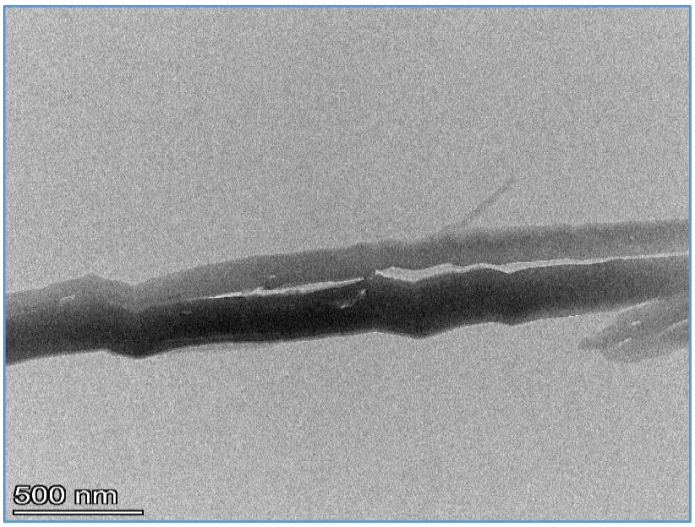

Figure 3: High Resolution Transmission Electron Microscopy of (BR-IONPs)

Table 1
Effect of BR-IONPs on A549 Cell Migration Distance at 0 h and 24 h Across Varying Concentrations

Concentrations	0 h	24 h
Control	2462.33 ± 25.54	958.67 ± 93.02
25 µg/mL	2521.30 ± 25.79	1054.67 ± 101.40
50 µg/mL	2478.33 ± 53.46	1533.67 ± 50.29
75 µg/mL	2489.67 ± 61.97	1906.33± 10.69
100 µg/mL	2438.00 ± 42.57	2035.67± 49.05
p-value	**<0.001***	**<0.001***

Table 2
Effect of BR-IONPs on H460 Cell Migration Distance at 0 h and 24 h Across Varying Concentrations

Concentrations	0 h	24 h
Control	2512.33 ± 25.54	1018.67 ± 93.02
25 µg/mL	2421.30 ± 25.79	1234.67 ± 101.40
50 µg/mL	25278.33 ± 53.46	1833.67 ± 50.29
75 µg//mL	2489.67 ± 61.97	1978.33± 10.69
100 µg/mL	2438.00 ± 42.57	2035.67± 49.05
p-value	**<0.001***	**<0.001***

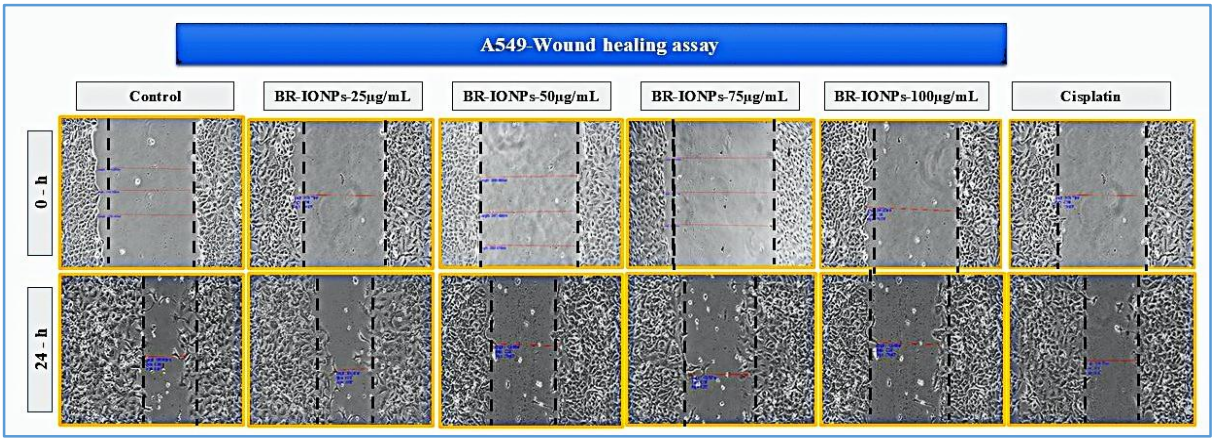

Figure 4: Wound Healing Assay of A549 Cells Treated with (BR-IONPs

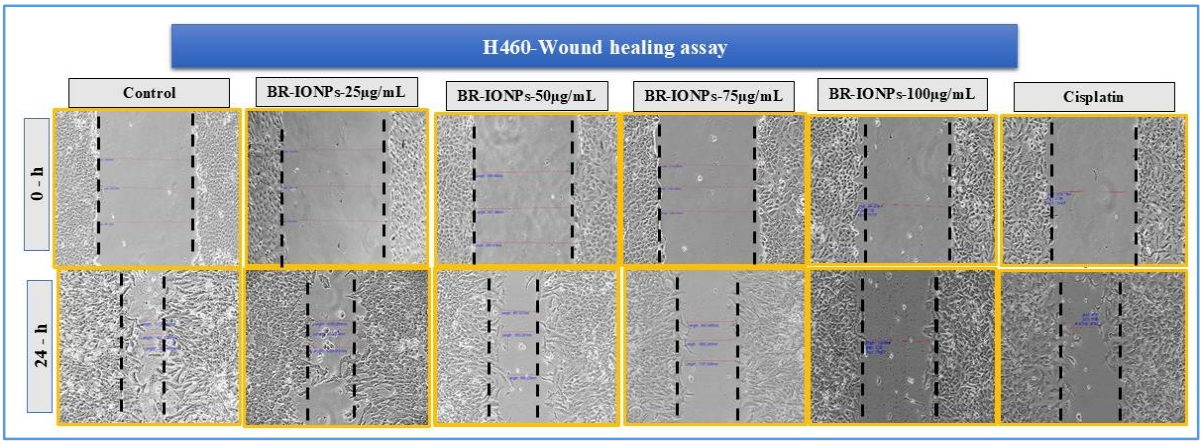

Figure 5: Wound Healing Assay of H460 Cells Treated with (BR-IONPs)

The present findings, along with previous studies, consistently demonstrate that berberine exerts a dose-dependent inhibitory effect on the migration of A549 lung cancer cells. Berberine-loaded liquid crystalline nanoparticles (Berberine-LCNs) significantly suppressed cell migration in both wound healing and Boyden chamber assays, highlighting the enhanced delivery potential of nanoparticle formulations[26]. Similarly, berberine-enriched copper oxide nanocomposites synthesized using *Solanum torvum* showed effective inhibition of A549 cell migration at 24 and 48 hours[31]. Moreover, free berberine at (30 µM) demonstrated strong anti-migratory effects on NSCLC[35].

Cytotoxic activity of BR-IONPs on A549, H460 NSCLC and HEK-293 cells: The cytotoxic effects of synthesized IONPs, BR, BR-IONPs and the standard chemotherapeutic drug cisplatin were assessed using the MTT assay on A549, H460 NSCLC and HEK-293 cell lines. The percentage of cell inhibition was measured at varying concentrations (0, 25, 50, 75 and 100 µg/mL). The results show that all drug dose-dependent cytotoxic effect was observed among all the drug concentrations in A549, H460 NSCLC cell lines. In A549 cells, IONPs exhibited cytotoxicity effects 15% at 25 µg/mL- 66% at 100 µg/mL and BR showed 28% at 25 µg/mL - 76% at 100 µg/mL. However, the combination of BR-IONPs produced greater inhibition 22% at 25 µg/mL - 83% at 100 µg/mL and cisplatin, a standard chemotherapeutic drug, showed 25% at 25 µg/mL- 69% at 100 µg/mL.

In H460 cells, similar results were observed: IONPs (16% at 25 µg/mL- 57% at 100 µg/mL) and BR (24% at 25 µg/mL- 66% at 100 µg/mL), while BR-IONPs again showed superior inhibition (27% at 25 µg/mL- 78% at 100 µg/mL) and cisplatin showed a comparable response (22% at 25 µg/mL- 69% at 100 µg/mL) respectively. In contrast, HEK-293 normal cells showed significantly lower inhibition with all test compounds. IONPs and BR exhibited moderate inhibition, ranging from 9% at 25 µg/mL - 22% at 100 µg/mL and 6% at 25 µg/mL - 19% at 100 µg/mL respectively. The BR-IONPs nanocomposite showed minimal toxicity, with inhibition between 3% at 25 µg/mL - 18% at 100 µg/mL. In contrast, cisplatin demonstrated higher cytotoxicity in HEK-293 cells, with inhibition ranging from 16% at 25 µg/mL - 63% at 100 µg/mL (Figure 6). The IC_{50} values for BR-IONPs, IONPs, BR and cisplatin are presented (Table 3).

Our results demonstrated that BR-IONPs exhibited significantly enhanced anticancer activity against A549 and H460 (NSCLC) cell lines compared to IONPs, BR and cisplatin. Importantly, BR-IONPs showed lower cytotoxicity towards normal HEK-293 cells while cisplatin caused the highest toxicity in these normal cells.

Table 3
IC_{50} Values of A549, H460 and HEK-293 cell lines

IC_{50} Values of Test Compounds in A549, H460 and HEK-293 Cells (24h)			
Test Compound	**A549 (µg/mL)**	**H460 (µg/mL)**	**HEK (µg/mL)**
IONPs	88.64±2.3	136.36±5.6	>200
Berberine (BR)	66.37±4.7	95.83±2.3	>200
BR-IONPs	54.76±1.4	69.23±3.1	>200
Cisplatin	68.43±1.2	92.14±2.3	107.14±3.1

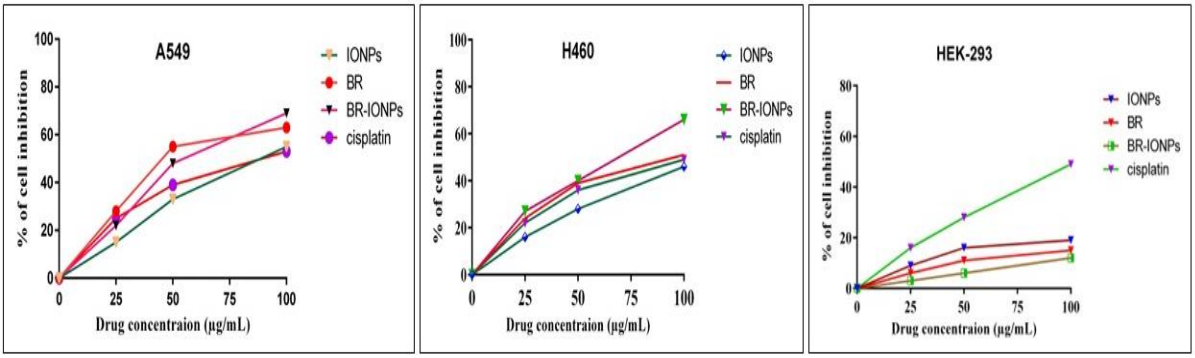

Figure 6: BR-IONPs Induce Dose-Dependent Cytotoxicity in A549 and H460 Lung Cancer Cells with Minimal Toxicity to HEK-293 cells

These findings were statistically significant with p-values < 0.05, indicating that BR-IONPs may offer a more effective and safer alternative for lung cancer treatment. Recent findings have demonstrated that FeONPs in A549 lung cancer cells reported a dose-dependent cytotoxic effect, with an IC_{50} value of 69 ± 0.50 µg/mL, indicating significant cytotoxicity at higher concentrations[5]. Similarly, berberine demonstrated a dose-dependent cytotoxic effect against HT29 colorectal cancer cells, with an IC_{50} of 52.37 ± 3.45 µM, indicating its ability to effectively suppress cell viability and to exhibit anticancer activity[20]. Furthermore, iron oxide nanoparticles synthesized using a facile flower extract were tested for their cytotoxic effect on MCF-7 and HEK-293 cell lines. The results revealed greater cytotoxic effects on MCF-7 cells compared to the HEK-293 cell line[32].

Conclusion

Our study concluded that BR-IONPs exhibit dose-dependent cytotoxic activity in A549 and H460 cancer cells, showing a significantly stronger anticancer effect compared to IONPs, BR, and cisplatin. Additionally, BR-IONPs demonstrate lower toxicity in the normal HEK-293 cell line compared to the chemotherapeutic drug cisplatin. It suggests their potential as a safe alternative for cancer treatment. Furthermore, BR-IONPs suppress the migration capacity of A549 and H460 cells, which may contribute to the prevention of metastasis. These findings highlight the promising therapeutic potential of BR-IONPs as an anticancer agent with selective cytotoxicity and reduced side effects.

References

1. Aisida S.O. et al, Biogenic synthesis of iron oxide nanorods using *Moringa oleifera* leaf extract for antibacterial applications, *Appl Nanosci (Switzerland)*, **10**, 305–315 **(2020)**

2. Attia N.F. et al, Iron oxide nanoparticles and their pharmaceutical applications, *Appl Surf Sci Adv*, **11**, 100284 **(2022)**

3. Adhikari A., Chhetri K., Acharya D., Pant B. and Adhikari A., Green synthesis of iron oxide nanoparticles using *Psidium guajava* L. leaves extract for degradation of organic dyes and anti-microbial applications, *Molecules*, **26(15)**, 4694 **(2021)**

4. Ashrafi-Saeidlou S., Rasouli-Sadaghiani M. and Fattahi M., Green synthesis of iron oxide nanoparticles using *Thymus migricus* for multifunctional applications in antioxidant, antimicrobial, photocatalytic and seed priming processes, *J Nanopart Res*, **27(1)**, 35 **(2025)**

5. Batool F. et al, Biologically synthesized iron nanoparticles (FeNPs) from *Phoenix dactylifera* have anti-bacterial activities, *Sci Rep*, **11**, 22132 **(2021)**

6. Bharathi D., Preethi S., Abarna K., Nithyasri M., Kishore P. and Deepika K., Bio-inspired synthesis of flower-shaped iron oxide nanoparticles (FeONPs) using phytochemicals of *Solanum lycopersicum* leaf extract for biomedical applications, *Biocatal Agric Biotechnol*, **27**, 101698 **(2020)**

7. Bray F. et al, Global cancer statistics 2022: GLOBOCAN estimates of incidence and mortality worldwide for 36 cancers in 185 countries, *CA Cancer J Clin*, **74**, 229-263 **(2024)**

8. Challaraj Emmanuel E.S., Mishra Arpita, Benny Suby Mon, Prince Amal and Joy Antony, Study on Desulfovibrio desulfuricans mediated copper corrosion and its inhibition using bio-wax of Colocasia esculenta, *Res. J. Chem. Environ.*, **28(4)**, 15-24 **(2024)**

9. Chang J.M. et al, Berberine derivatives suppress cellular proliferation and tumorigenesis *in vitro* in human non-small-cell lung cancer cells, *Int J Mol Sci*, **21**, 4218 **(2020)**

10. Chaturvedi V.K., Singh A., Singh V.K. and Singh M.P., Cancer nanotechnology: a new revolution for cancer diagnosis and therapy, *Curr Drug Metab*, **20**, 416-429 **(2018)**

11. Chaudhari R., Patel V. and Kumar A., Cutting-edge approaches for targeted drug delivery in breast cancer: beyond conventional therapies, *Nanoscale Adv*, **6**, 2270-2286 **(2024)**

12. Chen Q.Q. et al, Berberine induces apoptosis in non-small-cell lung cancer cells by upregulating miR-19a targeting tissue factor, *Cancer Manag Res*, **11**, 9005-9015 **(2019)**

13. Devarajan N. et al, Berberine A potent chemosensitizer and chemoprotector to conventional cancer therapies, *Phytother Res*, **35**, 3059-3077 **(2021)**

14. Devarajan N., Manjunathan R. and Ganesan S.K., Tumor hypoxia: The major culprit behind cisplatin resistance in cancer patients, *Crit Rev Oncol Hematol*, **162**, 103327 **(2021)**

15. Fatima E., Arooj I., Shahid H. and Aziz A., Characterization and applications of iron oxide nanoparticles synthesized from *Phyllanthus emblica* fruit extract, *PLoS One*, **19**, 0310728 **(2024)**

16. Han M.L., Zhao Y.F., Tan C.H., Xiong Y.J., Wang W.J. and Wu F., Cathepsin L upregulation-induced EMT phenotype is associated with the acquisition of cisplatin or paclitaxel resistance in A549 cells, *Acta Pharmacol Sin*, **37**, 1606-1622 **(2016)**

17. Hasan E. et al, A facile synthesis of iron oxide nanoparticles as a nano-sensor to detect levofloxacin and ciprofloxacin in human blood and evaluation of their biological activities, *RSC Adv*, **14**, 36093-36100 **(2024)**

18. Huang C., Liu H., Yang Y., He Y. and Shen W., Berberine suppressed the epithelial–mesenchymal transition (EMT) of colon epithelial cells through the TGF-β1/Smad and NF-κB pathways associated with miRNA-1269a, *Heliyon*, **10**, 36059 **(2024)**

19. Huang C., Wang X.L., Qi F.F. and Pang Z.L., Berberine inhibits epithelial-mesenchymal transition and promotes apoptosis of tumour-associated fibroblast-induced colonic epithelial cells through regulation of TGF-β signalling, *J Cell Commun Signal*, **14**, 53-66 **(2020)**

20. Li Q., Zhao H., Chen W. and Huang P., Berberine induces apoptosis and arrests the cell cycle in multiple cancer cell lines, *Arch Med Sci*, **19**, 1530–1537 **(2023)**

21. Lakshminarayanan S. et al, One-pot green synthesis of iron oxide nanoparticles from *Bauhinia tomentosa*: Characterization and application towards the synthesis of 1,3-diolein, *Sci Rep*, **11**, 8643 **(2021)**

22. Madhu G., Jaianand K., Rameshkumar K., Eyini M., Balaji P. and Veeramanikandan V., Solanum tuberosum extract mediated synthesis and characterization of iron oxide nanoparticles for their antibacterial and antioxidant activity, *J Drug Deliv Ther*, **9**, 5-15 **(2019)**

23. Nguyen H.T., Pham T.N., Le A.T., Thuy N.T., Huy T.Q. and Nguyen T.T.T., Antibacterial activity of a berberine nanoformulation, *Beilstein J Nanotechnol*, **13**, 641-652 **(2022)**

24. Niraimathee V.A., Subha V., Ravindran R.S.E. and Renganathan S., Green synthesis of iron oxide nanoparticles from *Mimosa pudica* root extract, *Int J Adv Res*, **15**, 227–240 **(2016)**

25. Phogat A., Singh J. and Malik V., Pharmacological effects of berberine – a Chinese medicine, against xenobiotic toxicity, *Pharmacol Res Mod Chin Med*, **13**, 100507 **(2024)**

26. Paudel K.R. et al, Berberine-loaded liquid crystalline nanoparticles inhibit non-small cell lung cancer proliferation and migration *in vitro*, *Environ Sci Pollut Res Int*, **29**, 46830-46847 **(2022)**

27. Pammi S.S.S. and Giri A., *In vitro* cytotoxic activity of *Phyllanthus amarus* Schum. & Thonn, *World J Biol Pharm Health Sci*, **6**, 034042 **(2021)**

28. Shabbir M.A. et al, Synthesis of iron oxide nanoparticles from *Madhuca indica* plant extract and assessment of their cytotoxic, antioxidant, anti-inflammatory and anti-diabetic properties via different nano informatics approaches, *ACS Omega*, **8**, 33358-33366 **(2023)**

29. Shanmugam R., Tharani M., Abullais S.S., Patil S.R. and Karobari M.I., Black seed assisted synthesis, characterization, free radical scavenging, antimicrobial and anti-inflammatory activity of iron oxide nanoparticles, *BMC Complement Med Ther*, **24**, 241 **(2024)**

30. Szliszka E., Czuba Z.P., Domino M., Mazur B., Zydowicz G. and Krol W., Ethanolic extract of propolis (EEP) enhances the apoptosis-inducing potential of TRAIL in cancer cells, *Molecules*, **14**, 738–754 **(2009)**

31. Sakthivel M.B. et al, Berberine-enriched copper oxide nano formulation synthesized using *Solanum torvum*: A strategic advancement in lung cancer therapy and wound healing, *J Appl Pharm Sci*, **15(6)**, 096-114 **(2025)**

32. Tabassum N., Singh V., Chaturvedi V.K., Vamanu E. and Singh M.P., A facile synthesis of flower-like iron oxide nanoparticles and its efficacy measurements for antibacterial, cytotoxicity and antioxidant activity, *Pharmaceutics*, **15**, 1726 **(2023)**

33. Tarawneh N., Hamadneh L., Abu-Irmaileh B., Shraideh Z., Bustanji Y. and Abdalla S., Berberine inhibited growth and migration of human colon cancer cell lines by increasing phosphatase and tensin and inhibiting aquaporins 1, 3 and 5 expressions, *Molecules*, **28**, 3797 **(2023)**

34. Viju Kumar V.G. and Prem A.A., Green synthesis and characterization of iron oxide nanoparticles using *Phyllanthus niruri* extract, *Orient J Chem*, **34**, 2583-2589 **(2018)**

35. Zhao X. et al, Berberine diminishes the malignant progression of non-small cell lung cancer cells by targeting CDCA5 and CCNA2, *J Nat Med*, **79**, 530-542 **(2025)**.

(Received 18th May 2025, accepted 23rd June 2025)